Inorg. Chem. **2003**, *42*, 5537–5544

Inorganic Chemistry
Article

# Dimerization of A-α-$[SiNb_3W_9O_{40}]^{7-}$ by pH-Controlled Formation of Individual Nb–*μ*-O–Nb Linkages

**Gyu-Shik Kim,[†] Huadong Zeng,[‡] Wade A. Neiwert, Jennifer J. Cowan,[§] Donald VanDerveer,[∥] Craig L. Hill,* and Ira A. Weinstock***

*Department of Chemistry, 1515 Pierce Drive, Emory University, Atlanta, Georgia 30322*

Received February 18, 2003

The reversible, stepwise formation of individual Nb–*μ*-O–Nb linkages during acid condensation of 2 equiv of A-α-$[SiNb_3W_9O_{40}]^{7-}$ (**1**) to the tri-*μ*-oxo-bridged structure A-α-$[Si_2Nb_6W_{18}O_{77}]^{8-}$ (**4**) is demonstrated by a combination of X-ray crystallography and variable-pD solution $^{183}$W and $^{29}$Si NMR spectroscopy. Addition of DCl to a pD 8.4 solution of **1** ($Li^+$ salt in $D_2O$) results in formation of a mono-Nb–*μ*-O–Nb-linked dimer, A-α-$[Si_2Nb_6W_{18}O_{79}]^{12-}$ (**2**; pD = 3.0–1.3). At pD values between 1.6 and 0.3, two isomers (*syn* and *anti*) of the di-*μ*-oxo-bridged dimer, A-α-$[Si_2Nb_6W_{18}O_{78}]^{10-}$ (**3**), are observed by $^{183}$W NMR ($C_{2v}$ and $C_{2h}$ symmetry for the *syn* and *anti* isomers, respectively; 5 $^{183}$W NMR signals for each isomer in the ratio 2:2:2:2:1). X-ray-quality crystals of *syn*-**3** were isolated in 53% yield (*syn*-A-α-$Cs_8H_2[Si_2Nb_6W_{18}O_{78}]\cdot 18H_2O$, orthorhombic, *Cmcm*, $a = 40.847(2)$, $b = 13.2130(7)$, and $c = 16.8179(9)$ Å at 173K, $Z = 4$, final $R_1 = 0.0685$). At the low-pD limit of –0.08 (1.2 M DCl), **4** alone is observed. Additional supporting data are provided by variable-pD $^{29}$Si NMR spectroscopy. Reversibility of the above processes was subsequently demonstrated by acquisition of $^{183}$W NMR spectra after incremental additions of LiOH to $D_2O$ solutions of **4** to effect its stepwise hydrolysis to 2 equiv of **1**.

## Introduction

The use of polyoxometalate (POM) cluster anions as nanoscale building blocks in the rational self-assembly of "giant" (high-nuclearity) clusters[1] and of new inorganic materials[2−6] entails the controlled formation of individual metal−oxygen bonds between POM subunits. Details of this general and fundamental process are herein documented using a prototypical POM subunit, A-α-$[SiNb_3W_9O_{40}]^{7-}$ (**1**).

In mixed tungstoniobate isopolyanions and in heteropolyanions such as **1**, the oxygen atoms in oxoniobium(V) (Nb═O) moieties are more basic and reactive than their oxotungsten(VI) (W═O) counterparts.[7−15] The greater reactivity of niobium oxygen bonds has been used to selectively form Nb−*μ*-O−Nb linkages between mixed-addendum hexam-

---

* To whom correspondence should be addressed. E-mail: iaweinst@wisc.edu (I.A.W.); chill@emory.edu (C.L.H.). I.A.W. is a visiting scientist at Emory University. Permanent address: USDA Forest Service, Forest Products Laboratory, Madison, WI 53705.

[†] Current address: Division of Science Education, College of Education, Kangwon National University, 192-1 Hyoja-2-dong, Chunchon, 200-701, Republic of Korea. We are sad to inform readers that Dr. Gyu-Shik Kim, our friend and colleague, passed away following an extended illness while this manuscript was in press.

[‡] Current address: NMR Core Facility, University of Alabama at Birmingham, 933 19th St., S. CH19B31, Birmingham, AL 35294.

[§] Current address: Institute of Paper and Science Technology, 500 10th Street, Atlanta, GA 30318.

[∥] Current address: Georgia Institute of Technology, X-ray Crystallography Laboratory, Atlanta, GA 30332.

(1) Kogerler, P.; Müller, A. In *Polyoxometalate Chemistry for Nano-Composite Design*; Yamase, T., Pope, M. T., Eds.; Kluwer Academic: New York, 2002; pp 1−16.
(2) Belai, N.; Dickman, M. H.; Kim, K.-C.; Ostuni, A.; Pope, M. T.; Sadakani, M.; Samonte, J. L.; Sazani, G.; Wassermann, K. In *Polyoxometalate Chemistry for Nano-Composite Design*; Yamase, T., Pope, M. T., Eds.; Kluwer Academic: New York, 2002; pp 17−26.
(3) Sanchez, C.; Soler-Illia, G. J. d. A. A.; Ribot, R.; Lalot, T.; Mayer, C. R.; Cabuil, V. *Chem. Mater.* **2001**, *13*, 3061−3083.
(4) Lin, Y.; Finke, R. G. *J. Am. Chem. Soc.* **1994**, *116*, 8335−8353.
(5) Aiken, I., John D.; Finke, R. G. *J. Am. Chem. Soc.* **1999**, *121*, 8803−8810.
(6) Johnson, B. J. S.; Stein, A. *Inorg. Chem.* **2001**, *40*, 801−808.
(7) Maestre, J. M.; Sarasa, J. P.; Bo, C.; Poblet, J. M. *Inorg. Chem.* **1998**, *37*, 3071−3077.
(8) Harrup, M. K.; Kim, G.-S.; Zeng, H.; Johnson, R. P.; VanDerveer, D.; Hill, C. L. *Inorg. Chem.* **1998**, *37*, 5550−5556.
(9) Judd, D. A.; Chen, Q.; Campana, C. F.; Hill, C. L. *J. Am. Chem. Soc.* **1997**, *119*, 5461−5462.
(10) Radkov, E.; Lu, Y. J.; Beer, R. H. *Inorg. Chem.* **1996**, *35*, 551.
(11) Lu, Y. J.; Lalancette, R.; Beer, R. H. *Inorg. Chem.* **1996**, *35*, 2524−2529.
(12) Kempf, J. Y.; Rohmer, M. M.; Poblet, J. M.; Bo, C.; Benard, M. *J. Am. Chem. Soc.* **1992**, *114*, 1136−1146.
(13) Edlund, D. J.; Saxton, R. J.; Lyon, D. K.; Finke, R. G. *Organometallics* **1988**, *7*, 1692−1704.
(14) Day, V. W.; Klemperer, W. G.; Schwartz, C. *J. Am. Chem. Soc.* **1987**, *109*, 6030−6044.
(15) Finke, R. G.; Rapko, B.; Saxton, R. J.; Domaille, P. J. *J. Am. Chem. Soc.* **1986**, *108*, 2947−2960.

10.1021/ic0341845 CCC: $25.00

etalate, Keggin, and Wells−Dawson anions.[8,11,13,14,16−19] Alternatively, in tungstoniobate clusters linked by Nb−$\mu$-O−Nb bonds, selective hydrolytic cleavage of the Nb−$\mu$-O−Nb linkages is observed.[11,13,14,16,19,20] In organic solvents, for example, A-$\beta$-$[Si_2Nb_6W_{18}O_{77}]^{8-}$ is cleanly (and reversibly) hydrolyzed to 2 equiv of monomeric A-$\beta$-$[SiNb_3W_9O_{40}]^{7-}$.[19] We similarly reported that, in $D_2O$ at pD = 7.4, complete hydrolysis of A-α-$[Si_2Nb_6W_{18}O_{77}]^{8-}$ (**4**) to 2 equiv of A-α-$[SiNb_3W_9O_{40}]^{7-}$ (**1**) occurs in less than 1 min at ambient temperature.[20] We now report the isolation and X-ray crystallographic characterization of the di-Nb−$\mu$-O−Nb-linked dimer, *syn*-A-α-$[Si_2Nb_6W_{18}O_{79}]^{10-}$ (*syn*-**3**), an intermediate in the condensation of **1** to **4**, which represents a previously unreported structural type. Variable-pD $^{183}W$ and $^{29}Si$ NMR spectroscopy are then used to document the sequential formation of individual Nb−$\mu$-O−Nb linkages that occurs during condensation of 2 equiv of **1** to **4**. To do this, it was necessary to find high-yield synthetic routes to water-soluble salts of **1** and **4**. Moreover, the use of A-α structures (rather than their A-$\beta$ analogues[19]) precluded complications that might otherwise have arisen from $\beta \rightarrow \alpha$ isomerization reactions.[21]

## Experimental Section

**Materials and Methods.** Tetra-*n*-butylammonium chloride ($Bu_4NCl$, TBACl), HCl, and DCl (37%, Aldrich), $Na_2WO_4{\cdot}2H_2O$ (AESAR), and $Nb_2O_5$ (AESAR) were obtained from commercial sources and used as received. All solvents were at least reagent grade and were used without further purification. A-α-$Na_{10}[SiW_9O_{34}]{\cdot}23H_2O$,[21] $K_7H[Nb_6O_{19}]{\cdot}13H_2O$,[22a,b] A-α-$(TBA)_6H_2[Si_2Nb_6W_{18}O_{77}]{\cdot}Et_2O$ ($(TBA)_6H_2$**4**$\cdot Et_2O$),[19] and A-α-$H_8[Si_2Nb_6W_{18}O_{77}]{\cdot}20H_2O$ ($H_8$**4**$\cdot 20H_2O$)[20] were prepared using literature methods. Infrared spectra were recorded on a Nicolet 510M FTIR spectrometer using either 3−5 wt % samples in KBr or as thin films deposited on a AgBr disk. FT Raman spectra of solid samples were obtained using a Nicolet Raman 950 spectrometer equipped with a germanium detector. Tungsten-183 NMR spectra (referenced to 2.0 M $Na_2WO_4$ in $D_2O$) were acquired at ambient temperature using an INOVAPlus 400 FT NMR spectrometer; $^{29}Si$ NMR spectra (referenced to 3.6 M TMS in $CDCl_3$) were acquired at ambient temperature using a UNITY 600 FT NMR instrument. C, H, and N analyses were performed by Atlantic Microlab Inc., Norcross, GA. Analyses of all other elements were performed by E+R Microanalytical Laboratory, Inc., Parsippany, NJ, or by Galbraith Laboratories Inc., Knoxville, TN.

**A-α-$Cs_6H[Si(NbO_2)_3W_9O_{37}]{\cdot}8H_2O$.** $K_7H[Nb_6O_{19}]{\cdot}13H_2O$ (1.91 g, 1.39 mmol) was dissolved in 250 mL of 0.5 M aqueous $H_2O_2$. To this stirred solution, 20 mL of 1.0 M aqueous HCl was added dropwise, to give a bright yellow solution, followed by addition of 7.82 g (2.72 mmol) of solid A-α-$Na_{10}[SiW_9O_{34}]{\cdot}23H_2O$. After the solid $Na_{10}[SiW_9O_{34}]$ had fully dissolved, 25.0 g (46.5 mmol) of solid CsCl was added to precipitate the Cs salt of A-α-$[Si(NbO_2)_3W_9O_{37}]^{7-}$, and the resulting orange yellow mixture was stirred for 15 min. The precipitate was filtered on a medium glass frit and washed with two 20-mL portions of diethyl ether. Drying in air gave 9.11 g of yellow powder (86.9% yield based on the hexaniobate precursor). Anal. Calcd (found) for $Cs_6H_{17}SiNb_3W_9O_{51}$: H, 0.48 (0.44); Si, 0.78 (0.62); Cs, 22.2 (21.9); Nb, 7.76 (7.50); W, 46.1 (46.5). FTIR (KBr, 1100−400 $cm^{-1}$): 994 (w), 957 (m), 903 (vs), 868 (sh), 789 (vs), 673 (vw), 592 (w), 534 (w). 482 (vw) $cm^{-1}$. $^{183}W$ NMR (0.1 M in $D_2O$) [$\delta$ (relative intensity)]: −111.4 (2W) and −138.4 (1W). See the Supporting Information (SI) for the preparation of the $(TBA)_4H_3$ salt.

**Synthesis of A-α-$Cs_7[SiNb_3W_9O_{40}]{\cdot}10H_2O$ ($Cs_7$1$\cdot 10H_2O$) from A-α-$Cs_6H[Si(NbO_2)_3W_9O_{37}]{\cdot}8H_2O$ ($Cs_6H$5$\cdot 8H_2O$).** Analytical and X-ray crystallographic data for $Cs_7$**1**$\cdot 10H_2O$ are given in ref 20; the preparation of $Cs_7$**1**$\cdot 10H_2O$ is reported here for the first time. A-α-$Cs_6H[Si(NbO_2)_3W_9O_{37}]{\cdot}8H_2O$ (4.50 g; 1.25 mmol) was dissolved in 150 mL of 0.5 M aqueous HCl. The yellow solution was refluxed for 2.5 h to give a colorless solution. At this stage of the synthesis, the solution contains condensed structures, which are subsequently hydrolyzed by the addition of CsOH to give $Cs_7$**1**. (As shown in the paragraph immediately below, **4** is a preferable starting material because it provides $Cs_7$**1**$\cdot 10H_2O$ in much higher yield.) The pH of the resulting solution was adjusted to 5 by dropwise addition of 6.0 M aqueous CsOH; a white precipitate was filtered off, and the filtrate was allowed to evaporate slowly in a fume hood. After 9 days, 0.70 g (15%) of crystalline solid was isolated. The following analytical data (from ref 20) are reproduced by permission of The Royal Society of Chemistry: Anal. Calcd (found) for $H_{20}Cs_7Nb_3O_{50}SiW_9$: Cs, 25.1 (24.7); Nb, 7.51 (7.40); W, 44.6 (45.0). FTIR (KBr, 1100−400 $cm^{-1}$): 1003 (w), 963 (m), 905 (s), 778 (vs), 538 (m). $^{183}W$ NMR (0.08 M in $D_2O$, +$LiClO_4$, −$CsClO_4$) [$\delta$ (relative intensity)]: −106.8 (2W), −148.7 (1W).

**Synthesis of A-α-$Cs_7[SiNb_3W_9O_{40}]{\cdot}10H_2O$ ($Cs_7$1$\cdot 10H_2O$) from A-α-$(TBA)_6H_2[Si_2Nb_6W_{18}O_{77}]{\cdot}Et_2O$ ($(TBA)_6H_2$4$\cdot Et_2O$).** This method provides $Cs_7$**1**$\cdot 10H_2O$ in much higher yield than does the method described above. CsOH (8.3 mL of a 1.0 M aqueous solution; 8.3 mmol) was added dropwise to a vigorously stirred acetonitrile solution of $(TBA)_6H_2$**4**$\cdot Et_2O$ (6.82 g, 1.03 mmol; in 60 mL of acetonitrile). During this time, a white solid precipitated and the heterogeneous solution was stirred for an additional 30 min. The white solid was filtered off and washed with methanol (2 × 20 mL) followed by diethyl ether (50 mL). Drying in air for 3 days gave a white powder (5.54 g, 1.49 mmol, yield 73.5%). The white powder ($Cs_7$**1**$\cdot 10H_2O$) was characterized by FTIR and $^{183}W$ NMR spectroscopic comparison with authentic samples prepared from A-α-$Cs_6H[Si(NbO_2)_3W_9O_{37}]{\cdot}8H_2O$ as described above. The water content (10 waters of hydration) was determined by thermogravimetric analysis: A weight loss of 4.84% was observed after heating at 200 °C for 5 h in a programmable electric oven.

**Synthesis of A-α-$Cs_7H[Si_2Nb_6W_{18}O_{77}]{\cdot}9H_2O$ ($Cs_7H$4$\cdot 9H_2O$) from $Cs_7$1$\cdot 10H_2O$.** $Cs_7$**1**$\cdot 10H_2O$ (3.80 g; 1.02 mmol) was dissolved in 160 mL of 2.0 M aqueous HCl, heated to 80 °C, filtered immediately, and placed in a fume hood in an open beaker. Slow evaporation for 5 days at ambient temperature gave 1.98 g of a colorless crystalline solid (60.8% yield). Anal. Calcd (found) for $H_{19}Cs_7Nb_6O_{86}Si_2W_{18}$: H, 0.31 (0.29); Cs, 14.9 (14.6); Nb, 8.92 (8.06); Si, 0.90 (0.84); W, 53.0 (52.9). FTIR (KBr, 1100−400 $cm^{-1}$): 1002 (sh), 977 (sh), 968 (w), 924 (s), 907 (sh), 787 (vs),

---

(16) Kim, G.-S.; Zeng, H.; VanDerveer, D.; Hill, C. L. *Angew. Chem., Int. Ed.* **1999**, *38*, 3205−3207.

(17) Kaba, M. S.; Song, I. K.; Duncan, D. C.; Hill, C. L.; Barteau, M. A. *Inorg. Chem.* **1998**, *37*, 398−406.

(18) Clegg, W.; Elsegood, M. R. J.; Errington, R. J.; Havelock, J. *J. Chem. Soc., Dalton Trans.* **1996**, 681−690

(19) Finke, R. G.; Droege, M. W. *J. Am. Chem. Soc.* **1984**, *106*, 7274−7277.

(20) Kim, G.; Zeng, H.; Rhule, J. T.; Weinstock, I. A.; Hill, C. L. *J. Chem. Soc., Chem. Commun.* **1999**, 1651−1652.

(21) Teze, A.; Herve, G. In *Inorganic Syntheses*; Ginsberg, A. P., Ed.; John Wiley and Sons, Inc.: New York, 1990; Vol. 27, pp 85−111.

(22) (a) Flynn, C. M.; Stucky, G. D. *Inorg. Chem.* **1969**, *8*, 178−180. (b) Filowitz, M.; Ho, R. K. C.; Klemperer, W. G.; Shum, W. *Inorg. Chem.* **1979**, *18*, 93−103. (c) Westcott, C. C. *pH Measurements*; Academic Press: New York, 1978. (d) Covington, A. K.; Paabo, M.; Robinson, R. A.; Bates, R. G. *Anal. Chem.* **1968**, *40*, 700−706.

**Table 1.** Summary of X-ray Crystallographic Data for *syn*-A-α-$Cs_8H_2[Si_2Nb_6W_{18}O_{78}]\cdot 18H_2O$ (*syn*-$Cs_8H_2\mathbf{3}\cdot 18H_2O$)

| | |
|---|---|
| empirical formula | $H_{38}Cs_8O_{96}Si_2Nb_6W_{18}$ |
| fw | 6560.22 |
| cryst color/shape | colorless thin plate |
| dimens, mm | 0.16 × 0.11 × 0.03 |
| cryst system | orthorhombic |
| space group | *Cmcm* (No. 63) |
| $T$, K | 173(2) |
| $a$, Å | 40.847(2) |
| $b$, Å | 13.2130(7) |
| $c$, Å | 16.8179(9) |
| $V$, Å$^3$ | 9076.7(8) |
| Z | 4 |
| $\rho_{calcd}$, Mg m$^{-3}$ | 4.804 |
| $F$(000) | 11 360 |
| $\mu$, mm$^{-1}$ | 26.742 |
| $\theta$ range, deg | 1.00−28.32 |
| no. of measd reflcns | 26 621 |
| no. of indep reflcns | 5733 |
| goodness of fit | 1.047 |
| final R$_1$ [$I > 2\sigma(I)$][a] | 0.0685 |
| final wR$_2$[b] | 0.1647 |

[a] $R_1 = \sum||F_o| - |F_c|/\sum|F_o||$. [b] $wR_2 = \{[\sum w(F_o^2 - F_c^2)^2]/\sum w(F_o^2)^2]\}^{1/2}$.

693 (s), 536 (w). FT Raman (1050−850 cm$^{-1}$): 998 (vs), 965 (sh), 940 (w), 910 (w). $^{183}$W NMR (0.08 M in $D_2O$, [$D^+$] = 1.2 M by addition of DCl; +$LiClO_4$, −$CsClO_4$) [$\delta$ (relative intensity)]: −124.1 (1W), −141.2 (2W). See the SI for the preparation of A-α-$Cs_8[Si_2Nb_6W_{18}O_{77}]\cdot 18H_2O$ ($Cs_8\mathbf{4}\cdot 18H_2O$) by cation exchange.

**Synthesis of *syn*-A-α-$Cs_8H_2[Si_2Nb_6W_{18}O_{78}]\cdot 18H_2O$ (*syn*-$Cs_8H_2\mathbf{3}\cdot 18H_2O$).** Yellow A-α-$Cs_6H[Si(NbO_2)_3W_9O_{37}]\cdot 8H_2O$ (0.42 g, 0.12 mmol) was dissolved in 10 mL of aqueous 0.5 M HCl. After removal of a small amount of insoluble solid by filtration through a fine glass frit, the yellow solution (filtrate) was refluxed until the color disappeared. The resulting colorless solution was allowed to evaporate in a hood for 3 days at room temperature, during which time very thin plate crystals formed. Isolation by filtration and drying in air gave 0.20 g of colorless thin plate crystals (52.8% yield). (The [$H^+$] at which these crystals are isolated from water corresponds to a pH of ca. 0.3, near the lower end of the range of pD values (ca. 0.3−1.6) at which **3** is observed by $^{183}$W NMR spectroscopy in $D_2O$.) Anal. Calcd (found) for $H_{38}Cs_8Nb_6O_{96}Si_2W_{18}$: Cs, 16.2 (16.8); Si, 0.86 (0.71); Nb, 8.50 (8.41); W, 50.4 (50.4). FTIR (KBr, 1100−400 cm$^{-1}$): 1005 (w), 967 (m), 917 (s), 783 (vs), 679 (s), 529 (w), 450 (vw), 423 (vw). FT Raman (1050−850 cm$^{-1}$): 997 (s), 982 (s), 934 (vw), 906 (vw), 861 (vs). A well-formed, colorless, thin-plate crystal with a size of 0.16 × 0.11 × 0.03 mm$^3$ was mounted on a glass fiber, and X-ray diffraction data were collected. The structure solution revealed the thin-plate crystal to be the *syn* isomer (Table 1). (See SI for experimental details on the data collection and refinement of *syn*-$Cs_8H_2\mathbf{3}\cdot 18H_2O$).

**Solution $^{183}$W NMR Observation of A-α-[$Si_2Nb_6W_{18}O_{78}$]$^{10-}$ (3).** Although *syn*-$Cs_8H_2\mathbf{3}\cdot 18H_2O$ has been structurally characterized and colorless crystals of this salt are stable indefinitely in the solid state, spectroscopic identification of **3** in $D_2O$ must nonetheless be approached with care. The need for caution derives from the fact that **3** contains terminal (Nb═O) and bridging (Nb−$\mu$-O−Nb) bonds, both of which are highly labile in water and sensitive to small changes in [$H^+$] (or [$D^+$]). As a result, $^{183}$W NMR spectra of this anion are not reliably obtained using solutions prepared by dissolution of crystalline *syn*-$Cs_8H_2\mathbf{3}\cdot 18H_2O$ in pure $D_2O$. Rather, spectroscopic identification of **3** in solution requires careful in-situ hydrolysis of a single Nb−$\mu$-O−Nb bond of **4** or partial condensation of **1**. Moreover, **3** exists in solution as an equilibrium (4:1 ratio) mixture of 2 isomers. At appropriate pD values, however, $^{183}$W NMR spectra of solutions of isomeric mixtures of **3** remain unchanged when acquired before and after weeks at room temperature. Thus, after the $^{183}$W NMR spectra of **1**, **2**, and **4** were first determined, the $^{183}$W NMR spectrum of **3** (mixture of 2 isomers) was established by repeated spectral acquisition over a range of pD values. In the hydrolysis of **4** (initially in 1.2 M DCl), the spectrum of **3** begins to appear at pD 0.3, followed (at pD 1.3) by signals associated with **2**. In the condensation of **1** (initially at pD values >7), signals associated with **2** appear at pD 1.9, and those associated with **3** appear at pD 1.6. It was thus determined that **3** is observed at pD values between ca. 1.6 to 0.3 and that its concentration is at a maximum (relative to **2** or **4**) at pD 0.8. Direct preparations of solutions suitable for $^{183}$W NMR spectroscopic observation of **3** are as follows:

**Method 1. Condensation of A-α-[$SiNb_3W_9O_{40}$]$^{7-}$ (1).** $Cs_7\mathbf{1}\cdot 10H_2O$ (1.98 g, 0.533 mmol) and $LiClO_4$ (0.60 g, 5.6 mmol) were dissolved in 3.0 mL of $D_2O$. After 30 min of stirring, solid $CsClO_4$ was removed by filtration. The pD of the solution was decreased by careful addition of 6.0 M DCl. Spectra were acquired at a series of pD values (see below), and at pD 0.76, two sets of signals, arising from two isomers of **3**, were observed by $^{183}$W NMR. Major isomer (5 signals): −98.4 (2W), −119.2 (2W), −129.4 (2W), −145.5 (1W), −147.4 (2W). Minor isomer (4 signals discernible): −101.5, −125.8, −130.8, −143.7.

**Method 2. Hydrolysis of A-α-[$Si_2Nb_6W_{18}O_{77}$]$^{8-}$ (4).** $Cs_8\mathbf{4}\cdot 18H_2O$ (1.0 g, 0.15 mmol) and 0.15 g (1.41 mmol) $LiClO_4$ were dissolved in 2.0 M DCl in $D_2O$ (3.6 mL), and solid $CsClO_4$ was removed by filtration. Prior to acquisition of $^{183}$W NMR spectra, the pD was 0.64. Two sets of signals, arising from two isomers of **3**, were observed by $^{183}$W NMR. Major isomer (5 signals): −101.2 (2W), −121.5 (2W), −130.0 (2W), −145.4 (1W), −146.8 (2W). Minor isomer (4 signals discernible): −102.7, −126.8, −131.3, −144.3. (Slight differences in these chemical-shift values, relative to the those observed in the condensation experiment above, are due to the different conditions: ionic strength values and $D^+$, $Li^+$, $Cl^-$, and POM-anion concentrations.)

**Variable-pD $^{183}$W NMR Spectroscopic Studies.**

**pD Measurements**. Reported pD values were obtained by applying a correction to pH readings displayed on an Orion model 250A pH meter equipped with a combination glass electrode. The relationship between pH-meter readings and actual pD values (at 24 °C) is pD = pH + 0.4.[22c,d] This formula applies when the $H_2O$-containing electrode of a typical pH meter is calibrated using standard aqueous buffer solutions and then inserted into $D_2O$. The actual concentration of $D^+$ in the $D_2O$ solution is then calculated by addition of 0.4 to the pH-meter reading. Although HDO was present in all experiments, its concentrations relative to those of $D_2O$ (55.1 M at 25 °C) (and concentrations of "$HD_2O^+$" relative to those of "$D_3O^+$") were small.

**Addition of DCl to A-α-[$SiNb_3W_9O_{40}$] (1).** $Cs_7\mathbf{1}\cdot 10H_2O$ (1.98 g, 0.533 mmol) was dissolved along with $LiClO_4$ (0.60 g, 5.6 mmol) in 3.0 mL of $D_2O$. After 30 min of stirring, insoluble $CsClO_4$ was removed by filtration to give 4.0 mL of a 0.13 M solution of monomer, which was 1.4 M in $Li^+$ (5.6 mmol) and 0.48 M in $ClO_4^-$ (1.9 mmol); total ionic strength, $\mu$, was 4.2 M (molar-scale $\mu$ values are approximated by molal-scale values calculated using the Debye−Hückel expression, $0.5\Sigma z^2m$, with molar values used in place of molal, $m$, values). The solution pD was then adjusted to an initial value of 8.4 (at which **1** is known to be stable)[20] by careful addition of a small amount of LiOH (1.0 M in $D_2O$) solution. A $^{183}$W NMR spectrum was acquired to confirm that no decomposition of **1** had occurred. Then, careful, dropwise addition of DCl (6.0 M in $D_2O$) was used to decrease the pD of the solution to 3.4. At pD 3.4, the only signals observed in the $^{183}$W NMR spectrum were those associated with intact **1** [$\delta$ (relative intensity)]: −107.2 (2W), −148.9 (1W). Successive $^{183}$W NMR spectra were obtained at pD values of 1.9, 0.76, and 0.6 and at $[\mathrm{D^+}] = 1.2$ M (pD = −0.08). At pD = 1.9, 5 new signals were observed: −101.6 (2W), −109.8 (2W), −124.0 (2W), −134.6 (1W), −147.6 (2W). These were assigned to the mono-$\mu$-oxo complex, A-α-$[\mathrm{Si_2Nb_6W_{18}O_{79}}]^{12-}$ (**2**). At a pD value of 0.76, two new sets of signals are observed. These are assigned to 2 isomers of **3**. Major isomer (5 signals): −98.4 (2W), −119.2 (2W), −129.4 (2W), −145.5 (1W), −147.4 (2W). Minor isomer (4 signals discernible): −101.5, −125.8, −130.8, −143.7. At the largest $[\mathrm{D^+}]$ value studied (1.2 M $\mathrm{D^+}$), **4** alone is observed: −124.4 (1W), −141.6 (2W). (See $^{183}$W NMR spectra in the Results and Discussion.)

**Reversible (in Situ) Hydrolysis and Recondensation Reactions.** LiOH was used in the stepwise hydrolysis of A-α-$[\mathrm{Si_2Nb_6W_{18}O_{77}}]^{8-}$ (**4**) to 2 equiv of A-α-$[\mathrm{SiNb_3W_9O_{40}}]^{7-}$ (**1**). DCl was then used in the stepwise recondensation of **1** to **4**. During the hydrolysis and condensation reactions, mono- and di-$\mu$-oxo-bridged intermediates (**2** and **3**, respectively) were observed by $^{183}$W NMR. Effectively identical results were obtained when the full experiment—stepwise hydrolysis followed by recondensation—was carried out starting from the free acid $\mathrm{H_8}$**4**·$20\mathrm{H_2O}$ dissolved in $\mathrm{D_2O}$. Descriptions of these experiments, including concentrations of all species present and ionic strength values, are provided as Supporting Information.

**Variable-pD $^{29}$Si NMR Spectroscopic Studies.** $\mathrm{Cs_7}$**1**·$10\mathrm{H_2O}$ (1.98 g, 0.533 mmol) and $\mathrm{LiClO_4}$ (0.60 g, 5.6 mmol) were dissolved together in 3.0 mL of $\mathrm{D_2O}$, and insoluble $\mathrm{CsClO_4}$ was removed by filtration. The presence of **1** (pD = 7.8) was confirmed by $^{29}$Si NMR spectroscopy (a singlet at $\delta = -79.96$ ppm). The pD of the solution was then gradually decreased to −0.08 ($[\mathrm{D^+}] = 1.2$ M) by careful addition of DCl (5.8 M or 2.6 M in $\mathrm{D_2O}$), and $^{29}$Si NMR spectra were acquired at successively smaller pD values.

## Results and Discussion

We previously reported that dissolution of $\mathrm{H_8}$**4**·$20\mathrm{H_2O}$ in $\mathrm{D_2O}$ (buffered at pD 7.4) results in the immediate neutralization and rapid hydrolysis of **4** to give 2 equiv of **1** (eq 1).[20] Upon dissolution of 2 equiv of $\mathrm{Cs_7}$**1**·$10\mathrm{H_2O}$ in 2.0 M aqueous HCl, the reverse reaction (condensation of **4** to **1**; this work) gives $\mathrm{Cs_7H}$**4**·$9\mathrm{H_2O}$ as a colorless crystalline solid in 61% isolated yield (eq 2).

$$\underset{\mathrm{H_8}\mathbf{4}}{\text{A-}\alpha\text{-}\mathrm{H_8[(Si_2Nb_6W_{18}O_{77}]}} + 14\mathrm{OH^-} \rightarrow \underset{\mathbf{1}}{2\text{A-}\alpha\text{-}[\mathrm{SiNb_3W_9O_{40}}]^{7-}} + 11\mathrm{H_2O} \quad (1)$$

$$\underset{\mathrm{Cs_7}\mathbf{1}}{2\text{A-}\alpha\text{-}\mathrm{Cs_7[SiNb_3W_9O_{40}]}} + 7\mathrm{H^+} \rightarrow \underset{\mathrm{Cs_7H}\mathbf{4}}{\text{A-}\alpha\text{-}\mathrm{Cs_7H[Si_2Nb_6W_{18}O_{77}]}} + 3\mathrm{H_2O} + 7\mathrm{Cs^+} \quad (2)$$

We now use a combination of X-ray crystallography and variable-pD solution $^{183}$W and $^{29}$Si NMR spectroscopy to reveal the sequential and reversible formation of individual Nb−$\mu$-O−Nb linkages (eqs 3−5) that occurs during the condensation or hydrolysis reactions in eqs 1 and 2. (In eqs 3−5 the $\mu$-O atoms that bridge the 2 A-α-$(\mathrm{SiNb_3W_9O_{37}})^{1-}$ fragments are shown explicitly.)

$$\underset{\mathbf{1}}{2\text{A-}\alpha\text{-}[\mathrm{SiNb_3W_9O_{40}}]^{7-}} \xrightleftharpoons[-\mathrm{H_2O}]{+2\mathrm{H^+}} \underset{\mathbf{2}}{\text{A-}\alpha\text{-}[(\mathrm{SiNb_3W_9O_{39}})_2(\mu\text{-O})]^{12-}} \quad (3)$$

$$\underset{\mathbf{2}}{\text{A-}\alpha\text{-}[(\mathrm{SiNb_3W_9O_{39}})_2(\mu\text{-O})]^{12-}} \xrightleftharpoons[-\mathrm{H_2O}]{+2\mathrm{H^+}} \underset{\mathbf{3}}{\text{A-}\alpha\text{-}[(\mathrm{SiNb_3W_9O_{38}})_2(\mu\text{-O})_2]^{10-}} \quad (4)$$

$$\underset{\mathbf{3}}{\text{A-}\alpha\text{-}[(\mathrm{SiNb_3W_9O_{38}})_2(\mu\text{-O})_2]^{10-}} \xrightleftharpoons[-\mathrm{H_2O}]{+2\mathrm{H^+}} \underset{\mathbf{4}}{\text{A-}\alpha\text{-}[(\mathrm{SiNb_3W_9O_{37}})_2(\mu\text{-O})_3]^{8-}} \quad (5)$$

**Synthesis.** To accomplish this, high-yield routes from the triperoxo anion A-α-$[\mathrm{Si(NbO_2)_3W_9O_{37}}]^{7-}$ (**5**) to water-soluble $\mathrm{H^+}$ or $\mathrm{Cs^+}$ salts of **1** and **4** were developed (here and in previous work). (Before acquisition of $^{183}$W NMR spectra, the $\mathrm{Cs^+}$ salts are converted to highly soluble $\mathrm{Li^+}$ salts by addition of $\mathrm{LiClO_4}$.) Key synthetic steps and their yields are shown in Scheme 1 (previously reported steps are clearly indicated; X-ray crystal structures of A-α-$\mathrm{(TBA)_6H_2}$**4**·$\mathrm{Et_2O}$ and A-α-$\mathrm{Cs_7}$**1**·$10\mathrm{H_2O}$ have been reported).[20] Notably, the A-α structural form of $[\mathrm{Si(NbO_2)_3W_9O_{37}}]^{7-}$ is retained throughout all steps used to prepare **1** and **4** (Scheme 1).

**X-ray Crystallographic and FTIR Studies of Nb−*μ*-O−Nb Bond Formation.** Solution $^{183}$W NMR spectroscopic identification of intermediates in the conversion of **1** to **4** was facilitated by isolation and X-ray and FTIR structural characterization of the *syn* isomer of the di-$\mu$-oxo-linked dimer A-α-$\mathrm{Cs_8H_2[Si_2Nb_6W_{18}O_{78}]}$ (*syn*-$\mathrm{Cs_8H_2}$**3**·$18\mathrm{H_2O}$). Colorless crystals of *syn*-$\mathrm{Cs_8H_2}$**3**·$18\mathrm{H_2O}$ (Figure 1) were obtained in 52.8% yield by mild acid condensation of A-α-$[\mathrm{Si(NbO_2)_3W_9O_{37}}]^{7-}$ in water (see Experimental Section). The anion has $C_{2v}$ symmetry, with one crystallographically imposed mirror plane parallel to the long axis of the molecule and passing through Si(1), Nb(1), and W(2) and a second crystallographically imposed mirror plane perpendicular to the first one and passing through the oxygen atoms, O(20) and O(20a), in the two Nb−$\mu$-O−Nb linkages. Instead of three Nb−$\mu$-O−Nb linkages, as seen in tri-$\mu$-oxo dimers of which A-α-$[\mathrm{Si_2Nb_6W_{18}O_{77}}]^{8-}$ (**4**) is exemplary, *syn*-**3** possesses two terminal Nb═O bonds (1.73(2) Å) which are *syn* to one another (the W═O bonds are nearly identical in length, 1.705(15) Å). The distance between the terminal oxygen atoms of the two Nb═O moieties is 3.59 Å. Assuming a Shannon and Prewitt crystallographic radius of ca. 1.25 Å for each of these O atoms, the space between the O atoms in the two Nb═O moieties is ca. 1.1 Å. The values of the Nb−$\mu$-O−Nb bond angles (139.6(12)°; Table 2) lie within experimental uncertainty ($3\sigma$) of those in the tri-$\mu$-oxo dimer, **4** (average: 137.0(7)°).[20] At the same time, the dihedral angle between the two $\mathrm{SiNb_3W_9O_{38}}$ Keggin fragments in *syn*-**3**, defined as the angle between one plane containing Nb(2), Nb(2a), O(20), and O(20a) and another plane containing Nb(2b), Nb(2c), O(20), and O(20a), which intersect in a line that includes the $\mu$-O atoms of these linkages, is very small (6.4°). The analogous angles in the tri-$\mu$-oxo dimer, **4**, are

**Scheme 1**

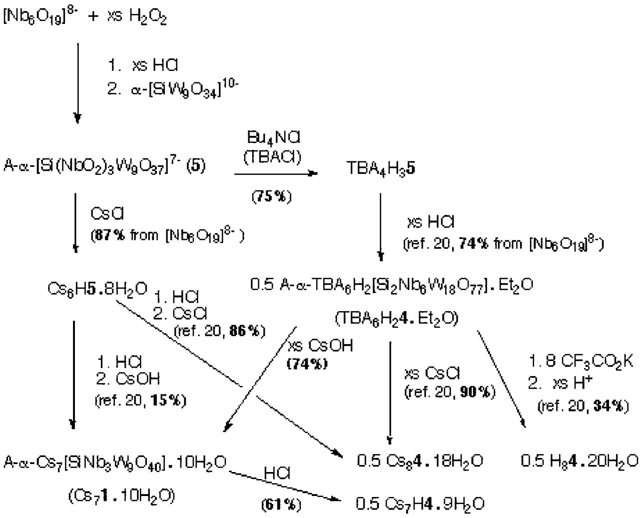

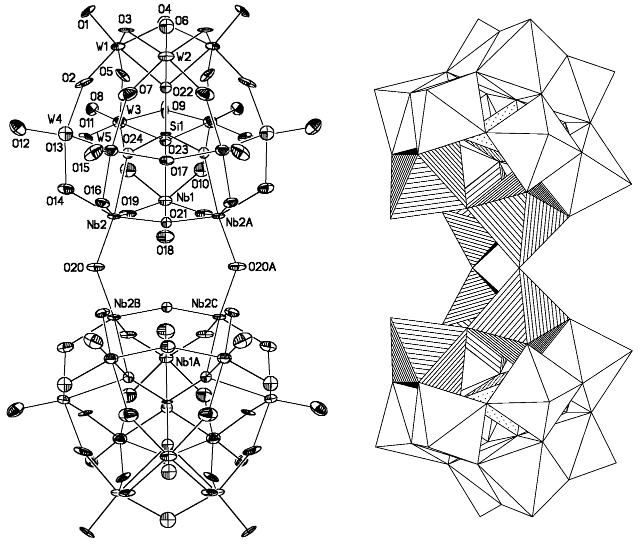

**Figure 1.** Structure of *syn*-A-α-$Cs_8H_2[Si_2Nb_6W_{18}O_{78}]$·$18H_2O$ (*syn*-**3**·$18H_2O$). Left: Thermal ellipsoid plot (50%). Right: Polyhedral representation after counterclockwise rotation of the structure shown on the left by ca. 90° around the long (vertical) axis.

**Table 2.** Selected Bond Lengths (Å) and Angles (deg) for *syn*-$Cs_8H_2$**3**·$18H_2O$

| | | | |
|---|---|---|---|
| | Distances | | |
| Nb(1)−O(18) | 1.73(2) | W(1)−O(1) | 1.699(14) |
| Nb(2)−O(14) | 1.981(14) | W(1)−O(2) | 1.866(14) |
| Nb(2)−O(19) | 1.856(12) | W(1)−O(3) | 1.922(13) |
| Nb(2)−O(20) | 1.905(7) | W(4)−O(14) | 1.866(13) |
| | Angles | | |
| Nb(1)−O(10)−W(3a) | 121.4(7) | W(1)−O(3)−W(2) | 121.2(6) |
| Nb(1)−O(19)−Nb(2) | 147.1(8) | W(1)−O(2)−W(4) | 151.2(7) |
| Nb(2)−O20)−Nb(2b) | 139.6(12) | W(3)−O(11)−W(4) | 152.7(8) |

22.3°. Notably, however, *syn*-**3** is related to the tri-*μ*-oxo dimer, **4**, by inversion of the two remaining Nb−*μ*-O−Nb linkages. The result of this inversion is that, upon hydrolysis of **4** to **3**, the dihedral angles that intersect at the O atoms of the two remaining Nb−*μ*-O−Nb linkages have “opened up” by 28.7° (this “opening up” of the structure is shown in the view at the right in Figure 1). Within the $SiNb_3W_9O_{38}$ fragments themselves, however, respective bond distances and angles in **3** and **4** are very similar to one another.[20]

FTIR spectra (solid samples in KBr) of **3** and **4** both possess characteristic Nb−*μ*-O−Nb stretching bands[11,13,14,16,19] in the 670−700 $cm^{-1}$ region (690 ± 3 $cm^{-1}$ for *syn*-$Cs_8H_2$**3**·$18H_2O$, 680 ± 3 $cm^{-1}$ for $Cs_8$**4**·$10H_2O$[20]). These values are also in line with the value of 690 $cm^{-1}$ reported for the single Nb−*μ*-O−Nb linkage between the two triniobium-capped Wells−Dawson anions in $[(P_2Nb_3W_{15}O_{61})(\mu\text{-}O)]^{16-}$.[13] These bands are absent, however, in FTIR spectra of the monomeric anions A-α-$[Si(NbO_2)_3W_9O_{37}]^{7-}$ and **1**.

**Variable-pD $^{183}$W and $^{29}$Si NMR Spectroscopic Studies. Observation of 1.** $Cs_7$**1**·$10H_2O$ (1.98 g, 0.533 mmol) and $LiClO_4$ (0.60 g, 5.6 mmol) were dissolved together in 3.0 mL of $D_2O$, insoluble $CsClO_4$ was removed by filtration, and the pD of the solution was adjusted to 8.4 by addition of aqueous LiOH (1.0 M in $D_2O$). The presence of intact **1** was confirmed by $^{183}$W NMR spectroscopy [*δ* (relative intensity)]: −106.8 (2W), −148.7 (1W). The pD of the solution was then gradually decreased by dropwise addition of DCl (6.0 M in $D_2O$). At a pD value of 3.4, **1** is still the dominant species present and the $^{183}$W NMR spectrum shown in Figure 2 (top) was obtained.

**Observation of 2.** As the pD of the solution is decreased further, the mono-*μ*-oxo complex, A-α-$[Si_2Nb_6W_{18}O_{79}]^{12-}$ (**2**), is the first new species observed. At pD = 1.9, five new $^{183}$W NMR signals (2:2:2:1:2 intensity ratios) are observed along with the two signals associated with **1** (Figure 2, pD = 1.9). The new signals are assigned to **2**, which possesses effective $C_{2v}$ symmetry.

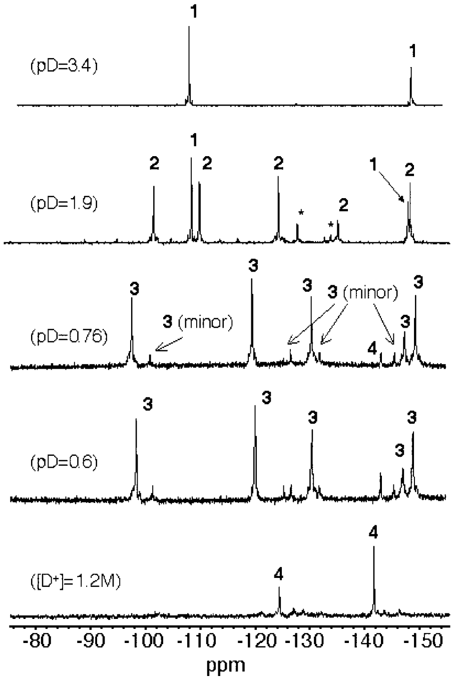

**Figure 2.** Variable-pD $^{183}$W NMR study of the step-wise condensation of **1** to **4**. Signals identified by asterisks are assigned to a minor byproduct, the tetrameric anion $[(Nb_4O_6)(A\text{-}\alpha\text{-}SiNb_3W_9O_{40})_4]^{20-}$.[16]

**Observation of 3.** At pD values of 0.76 and 0.60 ($[D^+]$ values of 0.17 and 0.25 M, respectively), signals associated with two isomers of **3** dominate the $^{183}$W NMR spectrum (Figure 2). Signals associated with **4** are now discernible and, while small, increase in intensity as the pD is decreased from 0.76 to 0.60. Notably, the relative intensities of the signals assigned to the minor isomer of **3** remain constant as the [D$^+$] is increased from 0.17 to 0.25 M. The major isomer of **3** gives rise to a set of 5 signals present in intensity ratios of 1:2:2:2:2. The presence of a minor isomer is indicated by the presence of 4 small signals. Both sets of signals are observed at pD values from ca. 0.3 to 1.6.

Five lines of evidence argue that the two sets of signals arise from closely related (*syn* and *anti*)[23] structural isomers of **3**. First, condensation of **3** (mixture of isomers) by addition of DCl gives **4**, while hydrolysis of **3** by addition of LiOH first gives the mono-$\mu$-oxo dimer, **2** (and no other compounds), and eventually **1**. Second, the two species present (isomers of **3**) are not related to one another by condensation or hydrolysis reactions: The relative concentrations (ratio of intensities of the two sets of signals) of the two anions remain fairly constant over the range of pD values (1.6−0.3) at which these signals are observed. This would not be true if the anions responsible for the two sets of signals were not structural isomers but, rather, were related to one another by hydrolysis or condensation reactions. Not only are such reactions rapid at room temperature, but the relative concentrations of condensation/hydrolysis products are sensitive to small changes in [D$^+$]. For example, while the relative concentrations of the isomers of **3** remain constant from pD 0.76 to pD 0.60, the concentration of **4** clearly increases (see Figure 2). Additionally, the relative concentrations of the isomers of **3** are the same whether solutions of **3** are prepared by condensation of **1** or by hydrolysis of **4**. Third, the IR spectrum of crystalline (structurally characterized) *syn*-$Cs_8H_2$**3**$\cdot 18H_2O$ is very similar to those of solid samples (concentrated reaction mixtures) containing both isomers of **3**. Fourth, the presence of *syn* and *anti* isomers of **3** is consistent with the numbers of signals observed for each isomer. The *syn* isomer, whose structure was determined by X-ray crystallography, has $C_{2v}$ symmetry; the *anti* isomer has $C_{2h}$ symmetry. Accordingly, both isomers should give rise to 5 signals with intensity ratios of 1:2:2:2:2. This is precisely what is observed for the major isomer. For the minor isomer, 4 signals are discernible, but their relative intensities are difficult to assess. Symmetry considerations, however, argue that the minor isomer must possess 5 chemically inequivalent W atoms: if the symmetry of this isomer were incrementally lower (i.e., $C_s$), rather than 5 signals (of which 4 are discernible), 10 signals would be expected. This is clearly not the case. The 5th line of evidence is provided by $^{29}$Si NMR (Figure 3).

At a pD value of 7.6, a single $^{29}$Si NMR signal, assigned to **1**, is observed at −79.96 ppm. At pD = 2.2, the intensity of this signal (due to monomeric **1**) is small, while that associated with mono-$\mu$-oxo **2** dominates (−79.78 ppm). A small-intensity signal due to di-$\mu$-oxo **3** is also observed ($\delta$ = −79.83 ppm). At a pD value of 1.1, **1** and **2** have effectively been condensed entirely to **3**, and its signal alone (−79.83 ppm) is observed. This is assigned to *syn*- and *anti*-**3** (the signals are either coincident or are averaged due to rapid isomerization on the $^{29}$Si NMR time scale). Further condensation results in formation of the tri-$\mu$-oxo dimer, **4** (−80.35 ppm), which is seen at a pD value of 0.30. (Note that at pD values of 1 and smaller, $^{29}$Si NMR signals gradually shift upfield. This is due to deuteration of **3** and **4** (10− and 8− anions, respectively) at these high [D$^+$] values.[24]) At [D$^+$] = 1.2 M, **4** is clearly dominant (−81.06 ppm).

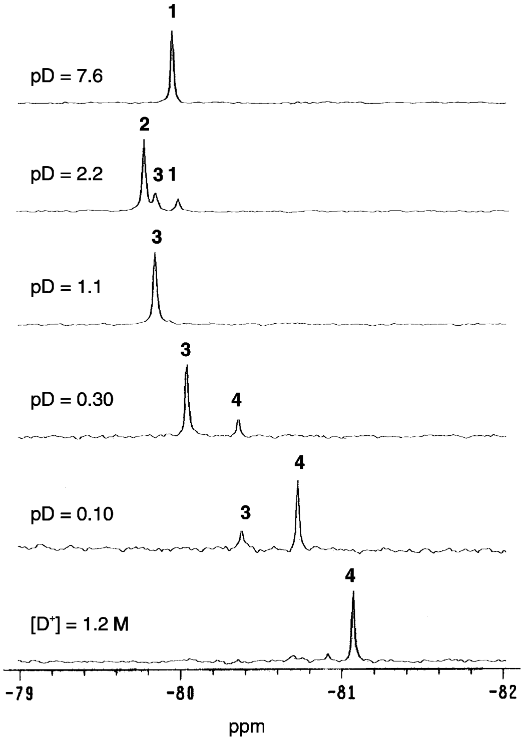

**Figure 3.** Variable-pD $^{29}$Si NMR study of the stepwise condensation of **1** to **4**. Upfield shift of the $^{29}$Si NMR signals of POMs at very low pD values (below 0.1 M D$^+$) is common and typically indicates deuteration of the cluster anions.[24]

These data provide an independent line of evidence that the two sets of $^{183}$W NMR signals assigned to **3** in Figure 2 arise from structural isomers (i.e., the isomers are *not* related to one another by condensation reactions). Moreover, the Si atoms in the minor isomer give rise to a single $^{29}$Si NMR signal. This indicates the presence of an axis of rotation that renders both $SiNb_3W_9O_{38}$ fragments chemically equivalent. This is consistent with the $C_{2h}$ symmetry of the *anti* isomer of **3**. All 5 lines of evidence demonstrate that the two sets of $^{183}$W NMR signals assigned to **3** (Figure 2) are due to structural isomers. Moreover, all data obtained are consistent with the presence of *syn* ($C_{2v}$) and *anti* ($C_{2h}$) isomers of **3**.[23]

The symmetries of these isomers are such that each structure gives rise to one $^{29}$Si and 5 $^{183}$W NMR signals. Therefore, neither NMR method can be used to establish which of the two isomers (*syn* or *anti*) is the dominant species observed in solution. Because morphologically homogeneous crystals of the structurally characterized *syn* isomer (*syn*-$Cs_8H_2$**3**$\cdot 18H_2O$) were isolated in 53% yield, it would be tempting to claim that the major isomer must therefore be

---

[23] Kirby, J. F.; Baker, L. C. W. *Inorg. Chem.* **1998**, *37*, 5537−5543.

[24] Pettersson, L.; Andersson, I.; Selling, A.; Grate, J. H. *Inorg. Chem.* **1994**, *33*, 982−993.

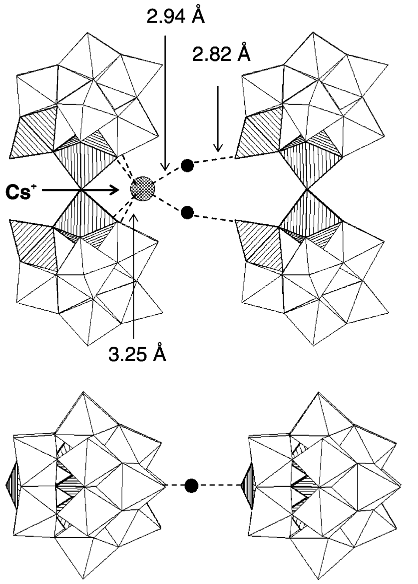

**Figure 4.** Crystal packing of *syn*-$Cs_8H_2$**3**·$18H_2O$. Octahedra with Nb(V) atoms at their centers are striped; W(VI)-centered octahedra are in white. The upper drawing shows the relative locations of a $Cs^+$ countercation (crosshatched circle) and water molecules (their O atoms are shown as small dark spheres) near the terminal Nb═O atoms. The lower drawing is rotated 90° out of the plane of the page to show the binding of the $Cs^+$ cation in the pocket created by inversion of the Nb−*μ*-O−Nb bridges between the two 2 $SiNb_3W_9O_{38}$ fragments.

*syn*. What prevents our doing so, however, is the fact that the isomers appear to be in equilibrium with one another in solution.[23,25−30] One indication of this is that the ratios of intensities of the sets of signals associated with each isomer (major or minor) are the same whether the isomer mixture is prepared by condensation of **2** or by hydrolysis of **4**.[25,27,29]

At the same time, analysis of the crystal lattice of *syn*-$Cs_8H_2$**3**·$18H_2O$ (Figure 4) suggests that the *syn* isomer (with a charge of 10−) might be selectively stabilized in solution by coordination to $Cs^+$. While extrapolation from solid-state structures to those in solution must be viewed with caution, we note that the "opened up" structure of *syn*-**3** provides a "pocket" for coordination to $Cs^+$. The topmost view in Figure 4 shows bonding distances (3.25 Å; 4 in all) between $Cs^+$ (crosshatched circle) and the *μ*-O atoms of Nb−*μ*-O−W linkages in the 2 $SiNb_3W_9O_{38}$ fragments. (The $Cs^+$ ion is also coordinated to the O atoms of 2 water molecules.) The bottom view shows how the $Cs^+$ cation is buried in the pocket created by the two $SiNb_3W_9O_{38}$ fragments. This pocket is unique to the inverted (opened up) structure of the *syn* isomer. In solution, selective association of $Cs^+$ with the pocket created by this inversion would be consistent with enhanced stabilization and, hence, a larger equilibrium concentration of the *syn* isomer. Note also that the terminal Nb═O atoms are hydrogen bonded to the H atoms (not shown) of the adjacent water molecules (small dark spheres). This supports arguments[31−33] that the terminal Nb═O bonds of the mono Nb−*μ*-O−Nb-bridged anhydride, [$(P_2W_{15}Nb_3O_{61})_2O$]$^{16-}$, [34,35] provide kinetic stability to Ir(0)[34,35] and Rh(0)[36] nanoparticles by electrostatic interaction between the POM anhydride and the electrophilic surfaces of late-transition-metal nanoparticles.

**Scheme 2**

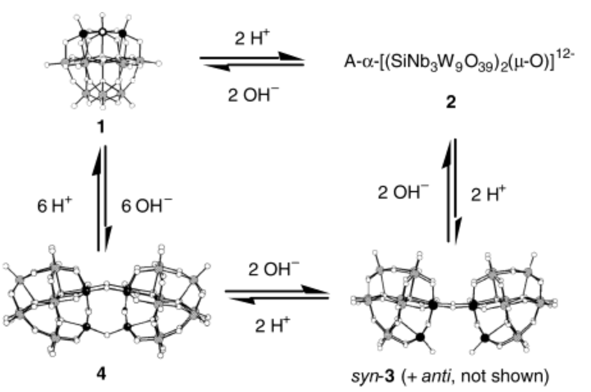

**Observation of 4.** When DCl is added to solutions containing *syn*- and *anti*-**3**, signals associated with both isomers decrease in intensity and two new signals are observed. Finally, at high [$D^+$] (1.2 M, pD = −0.08), **4** is the only anion observed (two $^{183}$W NMR signals, intensity ratios of 1:2; Figure 2).[20] As noted above, a single signal is observed in the $^{29}$Si NMR spectrum (Figure 3).

Finally, these processes are reversible: spectra acquired after incremental additions of LiOH to $D_2O$ solutions of **4** (hydrolysis of **4** to give **1**) are effectively identical to those acquired during subsequent condensation of **1** back to **4** (see details in the Supporting Information). Moreover, in the hydrolysis of **4**, spectra observed at each pD value studied (11 in all between pD −0.08 and 7.8) are effectively identical to those seen during the stepwise condensation of **1** to **4** shown in Figure 2. The results are summarized in Scheme 2 (structures shown were generated from X-ray crystallographic data).

## Conclusions

The use of POM cluster anions as nanoscale building blocks in the self-assembly of large structures and new inorganic materials entails the formation of metal−oxygen linkages between monomeric POM subunits. Details of this process are herein documented for the condensation of a prototypical POM subunit, A-α-[$SiNb_3W_9O_{40}$]$^{7-}$ (**1**; 2 equiv), to the tri-*μ*-oxo-bridged structure A-α-[$(SiNb_3W_9O_{37})_2$(*μ*-O)$_3$]$^{8-}$ (**4**). Intermediate mono- and di-*μ*-oxo-bridged structures (**2** and **3**) are observed by variable-pD $^{183}$W and $^{29}$Si

---

(25) Anderson, T. M.; Hill, C. L. *Inorg. Chem.* **2002**, *41*, 4252−4258.
(26) Neiwert, W. A.; Cowan, J. J.; Hardcastle, K. I.; Hill, C. L.; Weinstock, I. A. *Inorg. Chem.* **2002**, *41*, 6950−6952.
(27) Weinstock, I. A.; Barbuzzi, E. M. G.; Wemple, M. W.; Cowan, J. J.; Reiner, R. S.; Sonnen, D. M.; Heintz, R. A.; Bond, J. S.; Hill, C. L. *Nature* **2001**, *414*, 191−195.
(28) Cowan, J. J.; Bailey, A. J.; Heintz, R. A.; Do, B. T.; Hardcastle, K. I.; Hill, C. L.; Weinstock, I. A. *Inorg. Chem.* **2001**, *40*, 6666−6675.
(29) Weinstock, I. A.; Cowan, J. J.; Barbuzzi, E. M. G.; Zeng, H.; Hill, C. L. *J. Am. Chem. Soc.* **1999**, *121*, 4608−4617.
(30) Kim, K.-C.; Pope, M. T. *J. Am. Chem. Soc.* **1999**, *121*, 8512−8517.
(31) Widegren, J. A.; Finke, R. G. *J. Mol. Catal., A* **2003**, *191*, 187−207.
(32) Aiken, J. D., III.; Finke, R. G. *J. Mol. Catal., A* **1999**, *145*, 1−44.
(33) Aiken, J. D., III; Lin, Y.; Finke, R. G. *J. Mol. Catal., A* **1996**, *114*, 29−51.
(34) Lin, Y.; Finke, R. G. *J. Am. Chem. Soc.* **1994**, *116*, 8335−8353.
(35) Lin, Y.; Finke, R. G. *Inorg. Chem.* **1994**, *33*, 4891−4910.
(36) Aiken, J. D., III; Finke, R. G. *J. Am. Chem. Soc.* **1999**, *121*, 8803−8810.

NMR spectroscopy, and the *syn* isomer of **3**, a previously undocumented structural type, is characterized by X-ray crystallography. These data demonstrate the importance and potential utility of careful [$H^+$] control in the self-assembly of metal−oxide-bridged clusters, materials, and POM-stabilized transition-metal nanoclusters from POM building blocks.

**Acknowledgment.** We thank the DOE (Grant DE-FC36-95GO10090) (I.A.W. and C.L.H.) and the NSF (Grant CHE-9975453) (C.L.H.), the U.S. Army Research Office (Grant DAAD19-01-1-0593), and, in part, the Molecular Design Institute (Office of Naval Research, Grant N00014-95-1-1116) for support and Dr. Carl J. Houtman for FT-Raman spectra.

**Supporting Information Available:** Descriptions of variable-pD $^{183}$W NMR studies of reversible stepwise interconversions between **1** and **4**, tables listing crystal data and structure determination details, atomic coordinates and equivalent isotropic displacement coefficients, bond lengths and bond angles, and anisotropic displacement parameters for *syn*-$Cs_8H_2\mathbf{3}\cdot18H_2O$, and crystallographic data in CIF format for *syn*-$Cs_8H_2\mathbf{3}\cdot18H_2O$. This material is available free of charge via the Internet at http://pubs.acs.org.

IC0341845